Reconstruction of high sensitivity, stationary multi-pinhole cardiac SPECT data with analytical pinhole model

Haipeng Wang*, Hui Liu*, Yaqiang Liu* and Si Chen†,
*Department of Engineering Physics, Tsinghua University
Key Laboratory of Particle & Radiation Imaging
(Tsinghua University), Ministry of Education
Beijing, 100084, China.
†Beijing Novel Medical Equipment Ltd, Beijing, 100084, China.

***Abstract*—The conventional Dual-Head SPECT system for nuclear cardiac imaging suffered from low sensitivity. In this work we designed a high-sensitivity multi-pinhole SPECT system for dynamic studies. Two same flat collimators were placed with an angle 76°. The diameter of pinholes was 4.5 mm and the analytical calculation of sensitivity across $\sim$ 18 cm of FOV was 0.06%, four times higher than Dual-Head LEHR SPECT (typically 0.015%). The high sensitivity was at the cost of the spatial resolution, about 12 mm (analytical) in this design. To accomplish resolution recovery, a new analytical pinhole model was derived and a Gaussian model was used in calculation of the system matrix. Monte Carlo simulation of point source and myocardium phantom were performed with GATE. MLEM was used for reconstruction of simulation data with analytical pinhole model. The δ model was also used for comparison. The point projection images obtained from analytical pinhole model were compared with the ones obtained from long-time GATE simulation. The new pinhole model reduced the FWHM of point source reconstruction results from 11.7 $\times$ 10.9 $\times$ 10.2 mm^3 (Delta Model) to 3.4 $\times$ 3.7 $\times$ 3.0 mm^3. Myocardium phantom studies showed good performance and defect identification. In conclusion, this multi-pinhole dynamic SPECT system had high sensitivity and the resolution recovery was accomplished. In further work, this design will be implemented on variable-angle dual-head SPECT ImageE NET 632 and more studies will be performed.**

I. Introduction

The development of dedicated cardiac imaging has arose many attention in both research and industry field while most of the groups have adopted the design of SPECT with multi-pinhole collimators. Compared to the conventional rotational parallel-hole SPECT, the sensitivity of multi-pinhole SPECT could be improved with non-degraded spatial resolution, which allow diagnostic imaging in a very short time or reduce the injected doses. By using the expensive detectors, such as CZT, the commercial dedicated cardiac SPECT systems [1] [2] has highly improve the sensitivity and thus has the dynamic SPECT capabilities, however, it is not economical. For dynamic studies, the multi-pinhole SPECT is also a possible candidate in case the sensitivity is high enough. The previous studies have shown superior performance and better defect identification of proposed SPECT [3] [4] than the parallel-hole SPECT. Furthermore, in order to obtain higher sensitivity, the diameter of pinhole should be larger and the distance between source and detector should be smaller. The former will enlarge the projected area of point source and the latter will result in large angle of incidence near the border of detector. Consequently, the resolutionsensitivity trade-off must be well considered and the accurate modeling of system matrix will be more difficult.

In this study, we designed a high-sensitivity multi-pinhole cardiac SPECT system for dynamic studies, based on the clinical variable-angle dual-head SPECT ImageE NET 632. The diameter of pinholes was 4.5 mm. The analytical calculation of sensitivity across $\sim$ 18 cm of FOV was 0.06% that is approximately equal to commercial dynamical SPECT. To accomplish resolution recovery, a new analytical pinhole model was derived to calculate the system matrix. Monte Carlo simulation of point source and myocardium phantom were performed with GATE. Maximum Likelihood Estimation Method (MLEM) was used for reconstruction of simulation data with the new pinhole model. For comparison, the δ model was also used in reconstruction. The point projection images obtained from analytical pinhole model were compared with the ones obtained from long-time GATE simulation and they matched well. The point source study demonstrated the new analytical Gaussian model is valid for resolution recovery. Myocardium phantom studies showed better performance and defect identification.

II. Materials & Methods

A. System description

The design of multi-pinhole collimators is based on the clinical variable-angle dual-head SPECT ImageE NET 632, as described in Ref [4]. Each head has one single monolithic NaI(Tl) detector. The sensitivity area of each detector is 530 $\times$ 420 mm^2 and the intrinsic spatial resolution is 3.3 mm. The energy resolution for ^{99m}Tc 140 keV photons is better than 9.5%.

As shown in Fig. 1, two same flat collimators are placed with an angle 76°. The distance between collimator and the center of field of view (FOV) is 200 mm. All the pinholes focus on a FOV which is approximately a sphere of 18 cm

DOI: 10.12059/Fully3D.2017-11-3203035

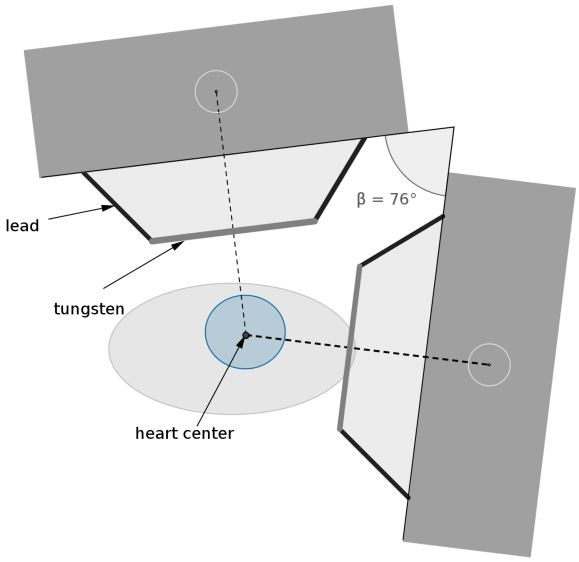

Fig. 1. The detector geometry of multi-pinhole SPECT system.

diameter. Each collimator has 12 pinholes and the opening angle of all the pinholes are designed differently to make sure the pinhole view all the FOV while the range are $42° \sim 49°$. The position of each pinhole is calculated to minimize the overlap of FOV projection. The diameters of pinholes are 4.5 mm. The sensitivity map was calculated using the formula in Ref [5]. The average resolution is calculated as the average of all pinholes' resolution weighted by each pinhole's sensitivity.

B. Analytical derivation of system matrix

For large pinhole diameter and large angle of incidence, we derived a new analytical pinhole model. In general, we consider a point source at S (x_s, y_s, z_s), a pinhole located at O $(0, 0, 0)$ and a projection plane at z = D, as shown in Fig. 2. The edge of a pinhole can be described with an equation

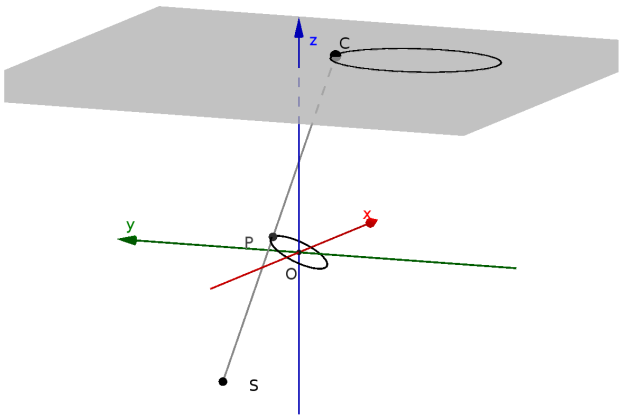

Fig. 2. Illustration of point projection through a large pinhole.

of circle, just as Eq. 1.

$$x^2 + y^2 + z^2 = r^2; z = y \cdot tan\theta \tag{1}$$

Besides, in Fig. 2, P (x_p, y_p, z_p) is an arbitrary point on the circle and C (x_c, y_c, z_c) is the intersect point C (x_c, y_c, z_c) between line SP and plane z=D. Then we can get the coordinates of point C,

$$x_c = x_s + \frac{(x_p - x_s)(D - z_s)}{(z_p - z_s)} \tag{2}$$

$$y_c = y_s + \frac{(y_p - y_s)(D - z_s)}{(z_p - z_s)} \tag{3}$$

$$z_c = z_s + \frac{(z_p - z_s)(D - z_s)}{(z_p - z_s)} = D \tag{4}$$

On the basis of Eq. (1-4), after some tedious derivations we demonstrate that the projection of circle described in Eq. 1 is exact an ellipse and its equation is

$$\lambda_{xx}x_c^2 + \lambda_{yy}y_c^2 + \lambda_{xy}x_c y_c + \lambda_x x_c + \lambda_y y_c + \lambda_0 = 0 \tag{5}$$

where

$$\lambda_{xx} = t^2 \tag{6}$$

$$\lambda_{yy} = x_s^2 tan^2\theta + sec^2\theta z_s^2 - r^2 tan^2\theta \tag{7}$$

$$\lambda_{xy} = 2tx_s tan\theta \tag{8}$$

$$\lambda_x = -2tx_s D \tag{9}$$

$$\lambda_y = -2[x_s^2 D tan\theta + z_s y_s D sec^2\theta + (t - D)tan\theta r^2] \tag{10}$$

$$\lambda_0 = sec^2\theta y_s^2 D^2 + x_s^2 D^2 - (t - D)^2 r^2 \tag{11}$$

and $t = z_s - y_s tan\theta$. As shown in Fig. 3, such an ellipse can be described with five parameters: the center (x_0, y_0), the length of long (L_a) and short (L_b) axes and the slant angle (α). These parameters can be calculated analytically form Eq. 5. Furthermore, we assume the typical projection of one pinhole is Gaussian. Then, the element of system matrix corresponding to point S and point (x, y, D) can be obtained with 3 step:

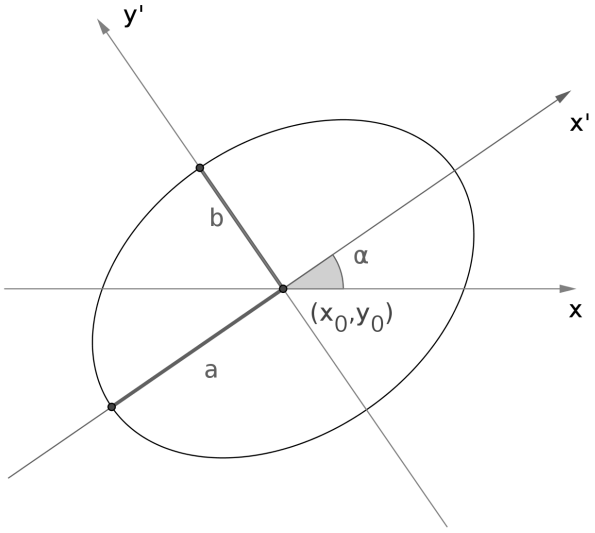

Fig. 3. The elliptical area of point projection. The ellipse is characterized by five parameters.

Step 1: Calculate the five parameters of S form Eq. 5

Step 2: Translate the x-y coordinate system to the center of ellipse and rotate the system with angle of α,

$$\begin{pmatrix} x' \\ y' \end{pmatrix} = \begin{pmatrix} cos\alpha & -sin\alpha \\ sin\alpha & cos\alpha \end{pmatrix} \begin{pmatrix} x - x_0 \\ y - y_0 \end{pmatrix} \tag{12}$$

Step 3: Calculate the value with Eq. 13

$$C(S; x, y) = A \times \epsilon \times I \times e^{-\lambda_1 \cdot ln2 \cdot (\frac{x'^2}{a^2} + \frac{y'^2}{b^2})} \tag{13}$$

$$I(x', y') = \begin{Bmatrix} 1 & when\ \frac{x'^2}{a^2} + \frac{y'^2}{b^2} < \lambda_2 \\ 0 & other \end{Bmatrix} \tag{14}$$

where ϵ is the sensitivity at point S, A is the constant of normalization and λ_1 & λ_2 are empirical parameters. As discussion in Ref [5], the effective diameter of pinhole is a little larger than the design diameter so the projected area is larger than the ellipse described in Fig. 3, thus λ_2 should be larger than 1.0. In this study λ_2 is about 3 and λ_1 is a little larger than 1.0. This analytical pinhole model allows calculation of system matrix on the fly.

C. Simulation and reconstruction

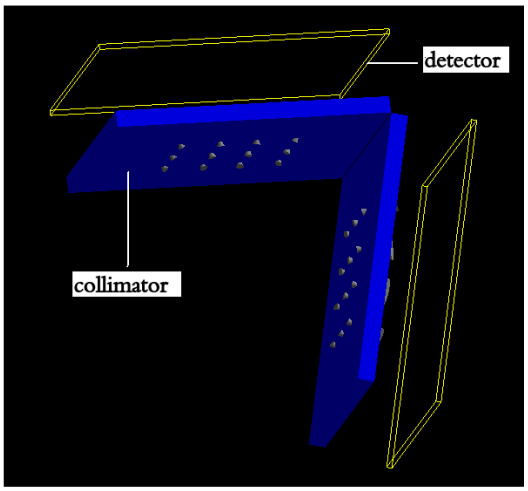

Fig. 4. Setup for SPECT system in GATE simulation.

As shown in Fig. 4, we implement this SPECT system in GATE for the MC simulation. First, one point source at the center of FOV was used in MC simulation and the simulation time was long enough. Two projections through different pinholes were used for analysis:

Projection 1: near the center of detector with small angle of incidence.

Projection 2: near the border of detector with large angle of incidence.

The two projections were also obtained analytically for comparison. Another MC simulation was performed with myocardium phantom of NCAT model. Besides, a defect with dimension 30×20×20 mm^3 were added in the phantom. The point source was reconstructed using MLEM with 50 iterative number and the myocardium phantom with 80 iterative number. The voxel's size was 4×4×4mm^3 and no filter is applied after the reconstruction. For comparison, two models were used in all above reconstruction:

a) δ Model: The pinhole and voxel are assumed to be point. The projection of one voxel through pinhole is δ function.

b) Analytical Gaussian Model: As discussion in Section II-B.

III. Results

The sensitivity map is shown in Fig. 5. The average sensitivity across the $\sim$ 18 cm FOV was 0.06%, higher enough than low energy high resolution (LEHR) parallel-hole SPECT (typically 0.015%) . Analytically, the spatial resolution is about 12 mm.

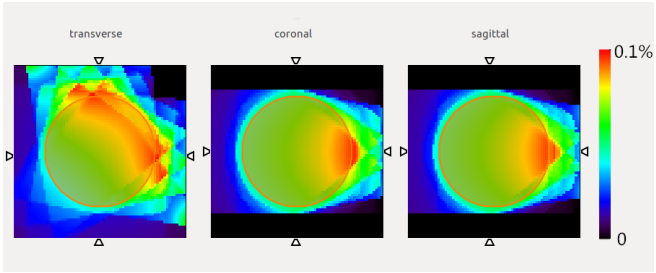

Fig. 5. The sensitivity map. The brown ellipsoid represents the targeted FOV.

As Fig. 6 shows, the point projections of ellipse pinhole model are compare with the simulation results. Both Projection 1 and Projection 2 match the GATE results well, especially the shape, indicating a good modeling of the pinhole.

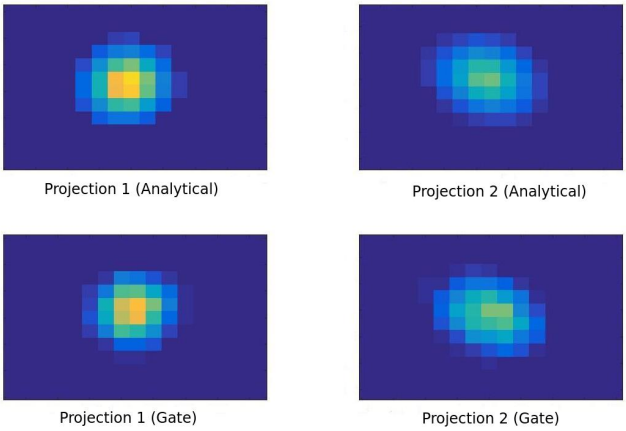

Fig. 6. Comparison of point projections between Analytical Gaussian Model and long-time GATE simulation.The pixel's size is 2 × 2 mm^2.

Fig. 7 shows the reconstruction results of point source using δ model and analytical Gaussian model. The Gaussian model was used to fit the image along different dimension and the fit results are list in Table.I. The result form analytical Gaussian model has obviously less deformation and small FWHM than δ model. Visibly, the result form analytical Gaussian model is

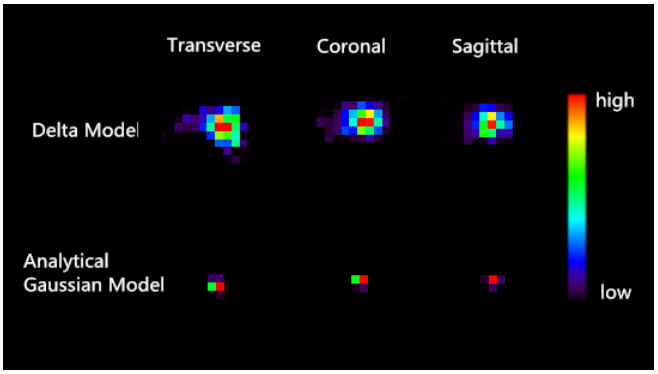

Fig. 7. The sample slices in three views of point source reconstruction images with different pinhole models. The voxel's size is $4 \times 4 \times 4$ mm^3.

TABLE I
FWHM OF POINT SOURCES RECONSTRUCTION RESULTS.

FWHM/mm	δ Model	Analytical Gaussian Model
x	11.7	3.4
y	10.9	3.7
z	10.2	3.0
$\sqrt{x^2+y^2+z^2}$	19.0	5.9

nearly in one voxel and about 4.0 mm spatial resolution could be achieved on the proposed SPECT system.

The results of myocardium phantom studies are shown in Fig. 8. About 0.6 M counts are acquired in the MC simulation and used for reconstruction. Unlike the multi pinhole SPECT with smaller diameter [4], the δ modeling can not give reasonable results for this proposed SPECT: visibly, the reconstruction image is bad and the defect is nearly unidentifiable. While, the main feature of myocardium phantom can be well reconstructed with analytical Gaussian model and the good defect identification is given.

IV. DISCUSSION&CONCLUSION

In this work we have proposed a novel design of the high sensitivity, stationary multi-pinhole cardiac SPECT with 0.06% sensitivity across $\sim$ 18 cm of FOV. Point source studies demonstrated the validation of new analytical Gaussian model and the resolution recovery is accomplished. The myocardium phantom studies have shown good performance and defect identification. In the future work, more proper phantom, including liver phantom, would be performed to evaluate the proposed SPECT system and the better reconstruction results are expected when prior information is added. The design will soon be implemented on variable-angle dual-head SPECT ImageE NET 632 and more studies on this multi-pinhole SPECT will be performed.

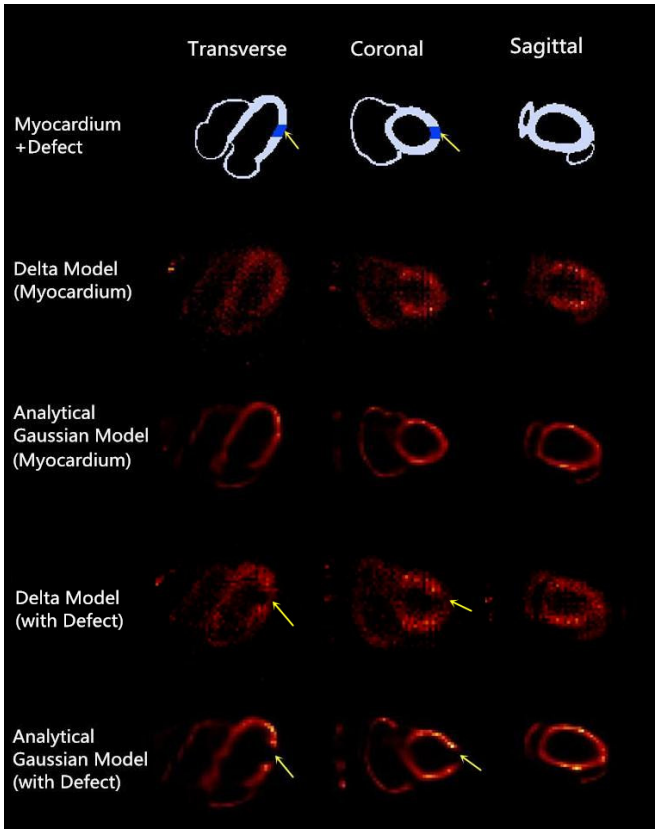

Fig. 8. Reconstruction results of the myocardium phantom with and without defect. The arrows mark the position of the defect.

REFERENCES

[1] E. V. Garcia, T. L. Faber, and F. P. Esteves, "Cardiac dedicated ultrafast spect cameras: new designs and clinical implications." *Journal of Nuclear Medicine*, vol. 52, no. 2, pp. 210–7, 2011.

[2] P. J. Slomka, J. A. Patton, D. S. Berman, and G. Germano, "Advances in technical aspects of myocardial perfusion spect imaging." *Journal of Nuclear Cardiology*, vol. 16, no. 2, pp. 255–276, 2009.

[3] H. Liu, S. Wang, T. Ma, J. Wu, S. Chen, Q. Wei, T. Dai, and Y. Liu, "Feasibility studies of a high sensitivity, stationary dedicated cardiac spect with multi-pinhole collimators on a clinical dual-head scanner," in *IEEE Nuclear Science Symposium and Medical Imaging Conference*, 2014, pp. 1–4.

[4] H. Liu, J. Wu, S. Chen, S. Wang, Y. Liu, and T. Ma, "Development of stationary dedicated cardiac spect with multi-pinhole collimators on a clinical scanner," in *IEEE Nuclear Science Symposium and Medical Imaging Conference*, 2015, pp. 1–4.

[5] S. D. Metzler and R. Accorsi, "Resolution- versus sensitivity-effective diameter in pinhole collimation: experimental verification." *Physics in Medicine & Biology*, vol. 50, no. 21, pp. 5005–17, 2005.